J Mater Sci (2008) 43:6952–6959
DOI 10.1007/s10853-008-2968-4

Creep deformation mechanism of magnesium-based alloys

Jingli Yan · Yangshan Sun · Feng Xue · Jing Bai · Shan Xue · Weijian Tao

Received: 22 July 2008 / Accepted: 22 August 2008 / Published online: 11 October 2008

Abstract Two heat-resistant magnesium alloys AJC421 and Mg-2Nd were prepared. Both as-cast Mg-2Nd and AJC421 alloys exhibited good creep resistance in comparison with commonly used magnesium alloys. The improvement in creep properties through Nd addition to pure magnesium is attributed to both solid solution and precipitation hardening. The stress exponents of 4.5–5.5 and activation energies of 70.0–96.0 kJ/mol obtained from the as-cast Mg-2Nd alloy at low temperatures and low stresses indicate the five power law can be used for predicting the creep mechanism. The additions of alkaline earth elements Sr and Ca into Mg–Al alloys suppress the discontinuous precipitation of $Mg_{17}Al_{12}$ and form thermal-stable intermediate phases at grain boundaries, leading to effective restriction to grain boundary sliding and migration. However, the mechanism responsible for creep deformation of Mg–Al based alloys with Ca and Sr additions is not consistent with the results of microstructure observations performed on the alloys before and after creep tests.

J. Yan · Y. Sun (✉) · F. Xue · J. Bai
Jiangsu Key Laboratory for Advanced Metallic Materials, Southeast University, Nanjing 211189, People's Republic of China
e-mail: yssun@seu.edu.cn

J. Yan
e-mail: jingly.yan@gmail.com

S. Xue
Ford Motor Research & Engineering (Nanjing) Co. Ltd., Nanjing 211100, People's Republic of China

W. Tao
Nanjing Welbow Metals Co. Ltd., Honglan, Nanjing 211221, People's Republic of China

Introduction

Magnesium alloys are of great interest as lightweight materials in automobile industry because of their low density and high specific strength and stiffness [1, 2]. However, compared with aluminum-based alloys, magnesium alloys have worse creep resistance at elevated temperatures, which limits their application only in a few selected components such as the instrument panel, steering wheel and valve cover [3]. The further applications of magnesium alloys in automobile industry such as power-train require good performance at elevated temperatures that may be up to 200–300 °C [1]. For automotive applications it is important that the development of new casting alloys addresses creep resistance, castability, especially die-castability, ductility, and corrosion resistance, besides, cost effectiveness should be taken into consideration as well [3, 4].

Concentrated effort has been expanded in developing and optimizing magnesium alloys with good creep resistance at elevated temperatures [1, 3–5]. Many creep-resistant magnesium alloys have been developed and some of them have been already commercially used (e.g., MRI, modified AE and AJ alloy systems). The heat-resistant magnesium alloys are commonly divided into two series, Al-free and Al-containing. The Al-free magnesium alloys often contain rare-earth elements such as Nd, Y, Ce, etc. These alloys offer good creep resistance due to solid solution and precipitation hardening. However, the application of these alloys is restricted in few areas such as space and aeronautics products owing to their poor castability and high cost. In comparison with Al-free alloys, the Al-containing magnesium alloys are the most hopeful candidates for application in automobile industry because of their good performance, die-castability, and low cost,

which is more important. Besides aluminum, the Al-containing creep-resistant magnesium alloys usually contain alkaline earth (Ca, Sr) or rare earth (misch metal) elements for better microstructure stability at elevated temperatures. The previous investigations [6] have attributed the poor elevated temperature performance of Mg–Al-based alloys to the discontinuous precipitation of β ($Mg_{17}Al_{12}$) from the supersaturated α-Mg solid solution and coarsening of β in the interdendritic eutectic regions at elevated temperatures. Creep resistance of Mg–Al-based alloy have been significantly improved by additions of alkaline elements because of the complete suppression of the formation of β phase and the presence, instead, of Al-Sr and/or Mg–Ca and Mg–Al-Sr ternary phase [6]. Mg-2Nd and AJC421 are two newly developed creep-resistant magnesium alloys. Although both the alloys exhibit good creep resistance, their castability and potential applications are different. Mg-2Nd-alloy with 2 wt.% Nd addition is usually for gravity casting applications and wrought products. However, AJC421 alloy is always considered as a structural material for die-casting applications due to good fluidity.

In the previous investigations the creep mechanisms of magnesium alloys were mostly identified by determining the apparent activation energy Q for creep as well as the stress exponent n from the Arrhenius relationship [1, 3]. However, more and more investigations [7, 8] have indicated that it has difficulties in inferring the mechanisms responsible for the creep deformation of h.c.p-structured magnesium alloys using the Arrhenius equation. In the present paper, two alloys, Al-containing alloy AJC421 (here, J represents Sr and C represents Ca) and Al-free alloy Mg-2Nd, were prepared. The creep behaviors of these two alloys were studied and the mechanism responsible for creep deformation of them was also investigated and compared.

Experimental procedure

Mg-2Nd and AJC421 with composition of Mg-4Al-2Sr-1Ca-0.3Mn were prepared. The additions of Nd, Sr, and Ca were conducted by adding master alloys of Mg-30 wt.%Nd, Mg-27 wt.%Sr, and Mg-30 wt.%Ca, respectively. Melting of the alloys was carried out in a mild steel crucible under the protection of a mixed gas atmosphere of 1% SF_6 and 99% CO_2. After the master alloy added was dissolved, the melt was held at 720 °C for 10 min and then poured into a water-cooled mold made of cast copper. The chemical compositions of the alloys prepared were determined by using inductively coupled plasma atomic emission spectroscopy (ICP) and the results were well consisted with the designed composition, as shown in Table 1.

Some of the cast ingots with 60 mm in diameter were hot extruded into 20 mm-thick bars at 360 °C. The as-cast and as-extruded specimens for creep tests were cut from the cast billets and extruded bars. Tensile-creep tests were performed on specimens of cylindrical geometry with a 100 mm gauge length and 10 mm diameter cross section using RD2-3 high temperature creep testing machine. Microstructure observations were carried out using optical microscopy (OM), scanning electron microscopy (SEM), and transmission electron microscopy (TEM). Microanalysis was performed on different phases in the microstructure using energy dispersive X-Ray spectroscopy (EDS). The crystalline structure of the precipitates appearing in the microstructure was characterized using selected area electron diffraction (SAD).

Results

Microstructure

The microstructure of the as-cast Mg-2Nd consists of the α-Mg matrix and an intermediate phase distributing discontinuously at grain boundaries, as shown in Fig. 1a. Figure 1b and c are TEM micrographs and corresponding electron diffraction pattern taken from the intermediate phase, which can be indexed as arising from $Mg_{12}Nd$ with a body-centered tetragonal structure. Dynamic recrystallization has also occurred in this alloy during extrusion process, as shown in Fig. 1d, optical micrograph taken from extruded alloy of Mg-2Nd along the longitudinal direction. The average grain size in extruded Mg-2Nd is about 5–20 μm. The intermediate phase $Mg_{12}Nd$ shows band morphology parallel to the extrusion direction as shown in Fig. 1e.

A SEM micrograph taken from as-cast AJC421 is shown in Fig. 2a, from which a network of interdendritic

Table 1 Chemical composition of the alloys

Alloys	Designed compositions (wt.%)						Analyzed compositions (wt.%)					
	Nd	Al	Sr	Ca	Mn	Mg	Nd	Al	Sr	Ca	Mn	Mg
Mg-2Nd	2.0	–	–	–	–	Bal.	1.85	–	–	–	–	Bal.
AJC421	–	4.0	2.0	1.0	0.3	Bal.	–	3.79	2.22	1.01	0.31	Bal.

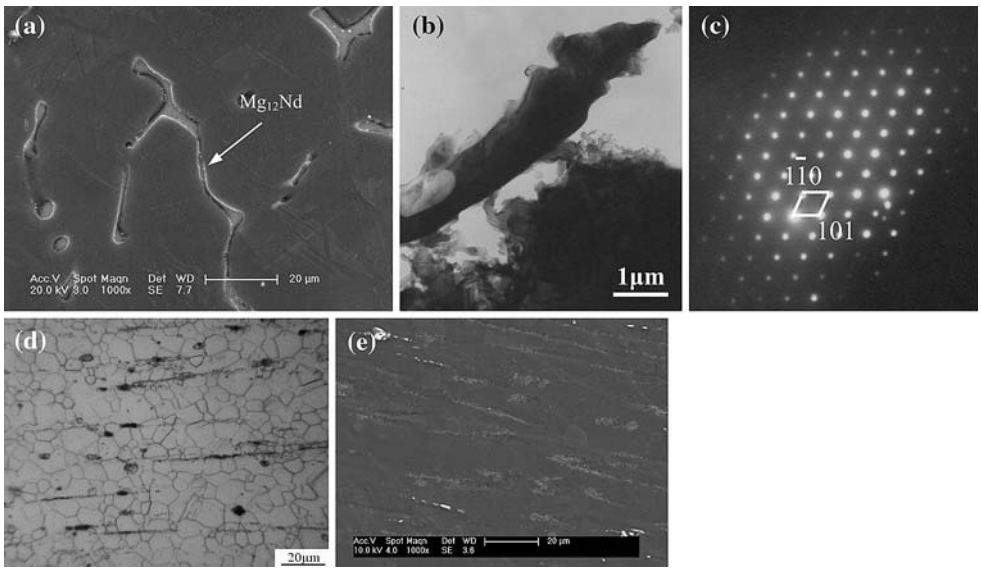

Fig. 1 (**a**) SEM, (**b**) TEM image, (**c**) selected area diffraction pattern (SADP) of as-cast Mg-2Nd (B = $11\bar{1}$), (**d**) optical, and (**e**) SEM morphology of as-extruded Mg-2Nd

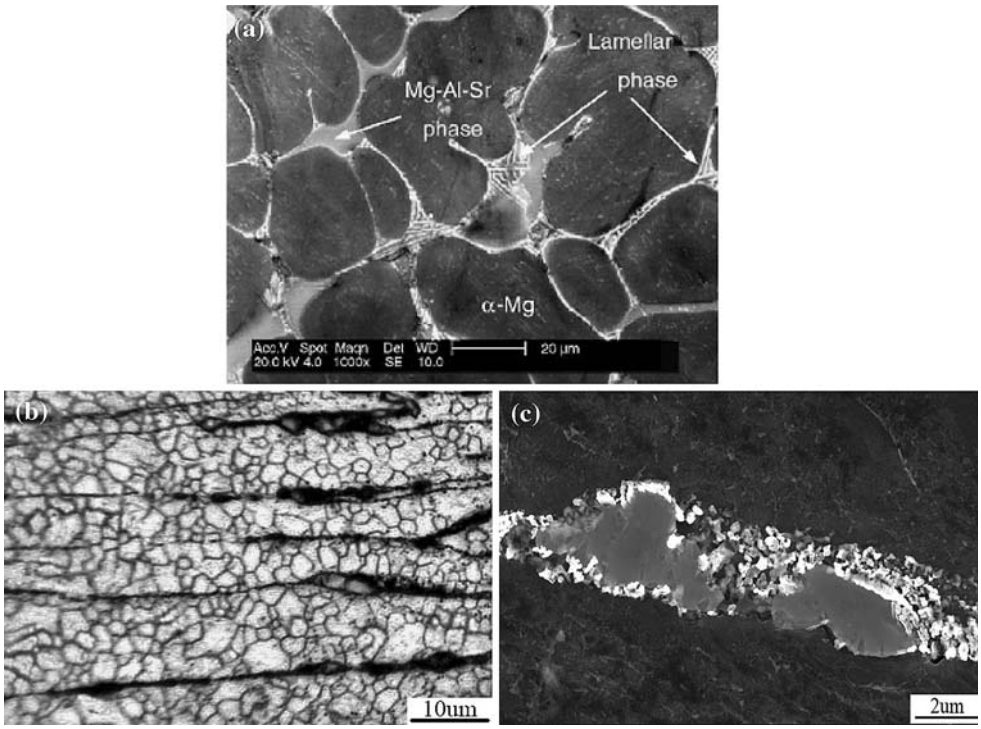

Fig. 2 (**a**) SEM micrograph of as-cast AJC421 alloy, (**b**) Optical, and (**c**) SEM micrograph of the extruded AJC421 alloy

compounds can be clearly seen. Our previous paper [6] reported that the interdendritic network in the alloy AJC421 consists of bulky Mg–Al-Sr ternary phases and lamellar eutectic Mg_2Ca or $(Mg, Al)_2Ca$ phases. While the alloy was extruded, its microstructure is similar to that of as-extruded Mg-2Nd alloy. As shown in Fig. 2b the grains of the α-Mg matrix are equiaxial and their average size is about 4 μm in diameter, indicating that recrystallization also occurred during extrusion. The intermediate phases in as-extruded microstructure are arranged in bands parallel to the extrusion direction. High magnification SEM observation, as shown in Fig. 2c, reveals that the ternary phase of Mg–Al-Sr is a little elongated in comparison with that in as-cast microstructure, while the Mg_2Ca or $(Mg, Al)_2Ca$ phases are crushed into a large amount of small particles.

Creep behavior

The creep behavior of the as-cast Mg-2Nd alloy was studied at temperatures between 150 and 250 °C under applied stresses between 30 and 110 MPa. Figure 3 shows

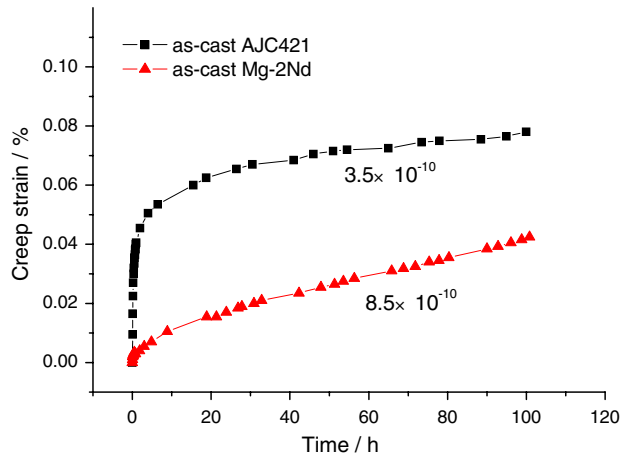

Fig. 3 Creep curves of the as-cast alloys Mg-2Nd and AJC421 at 175 °C/70 MPa

the creep curve obtained at the temperature of 175 °C and a constant stress of 70 MPa. The steady-state creep rate ($\dot{\varepsilon}$) calculated by measuring the slope of the steady-state stage of the curve is 8.5×10^{-10} s^{-1}. The 100 h total creep extensions (ε_t) is only 0.043%.

The steady-state secondary creep rate ($\dot{\varepsilon}$) of magnesium alloys is generally described by a power-law equation [1, 9, 10]

$$\dot{\varepsilon} = A\sigma^n \exp\left(\frac{-Q}{RT}\right) \quad (1)$$

where A is a material related constant, n is the stress exponent, Q is the apparent activate energy for creep, R is the gas constant. The Eq. 1 can be changed into

$$\ln \dot{\varepsilon} = \ln A + n \ln \sigma - \frac{-Q}{RT} \quad (2)$$

by taken logarithm at both sides. Thus, the stress exponent n can be calculated from the slope of $\ln \dot{\varepsilon}$ versus $\ln \sigma$ at a given temperature from the above Eq. 2, and an Arrhenius plot ($\ln \dot{\varepsilon}$ vs. $1/T$) at a specific stress level will yield the apparent activation energy (Q) value. The applied stress and temperature dependence of the steady-state creep rate of the as-cast Mg-2Nd alloy are shown in Fig. 4a and b, respectively. The stress exponents calculated from the double logarithmic plots of minimum creep rate against applied stress ($\ln \dot{\varepsilon}$ vs. $\ln \sigma$) lie in the range of 4.5–7.1 at low stresses and 9.8–29.5 at high stresses, as shown in Fig. 4a. The activation energies for creep calculated from the slope of the $\ln \dot{\varepsilon}$ vs. $1/T$ curve (Fig. 4b) can be divided into two parts: 70.0–96.0 kJ/mol at lower temperatures (150–200 °C) and 199.9–246.1 kJ/mol at higher temperatures (200–250 °C).

Creep tests of the as-cast AJC421 alloy were performed at temperatures between 150 and 250 °C under applied stresses between 50 and 80 MPa. The creep curve obtained at 175 °C/70 MPa is also shown in Fig. 3. The creep strain of AJC421 is larger than that of Mg-2Nd in the primary creep stage, which may be attributed to the difference in yield strength at 175 °C of the two alloys. The steady-state creep rate ($\dot{\varepsilon}$) is 3.5×10^{-10} s^{-1} and the 100 h total creep extensions (ε_t) is 0.078%. Both the steady creep rate and 100 h total creep extension are much lower than the commercial magnesium alloy AE42 ($\dot{\varepsilon} = 5.6 \times 10^{-8}$ s^{-1}, $\varepsilon_t = 2.96\%$) [11], indicating a better creep resistance. The relationship between the secondary creep rates and applied stress and the temperature dependence of the minimum creep rates are shown in Fig. 5a and b, respectively. The stress exponents are 4.4 at 175 °C/50–80 MPa and 4.7 at 200 °C/50–70 MPa, respectively. However, when the temperature is as high as 225 °C, the stress exponent is 6.6

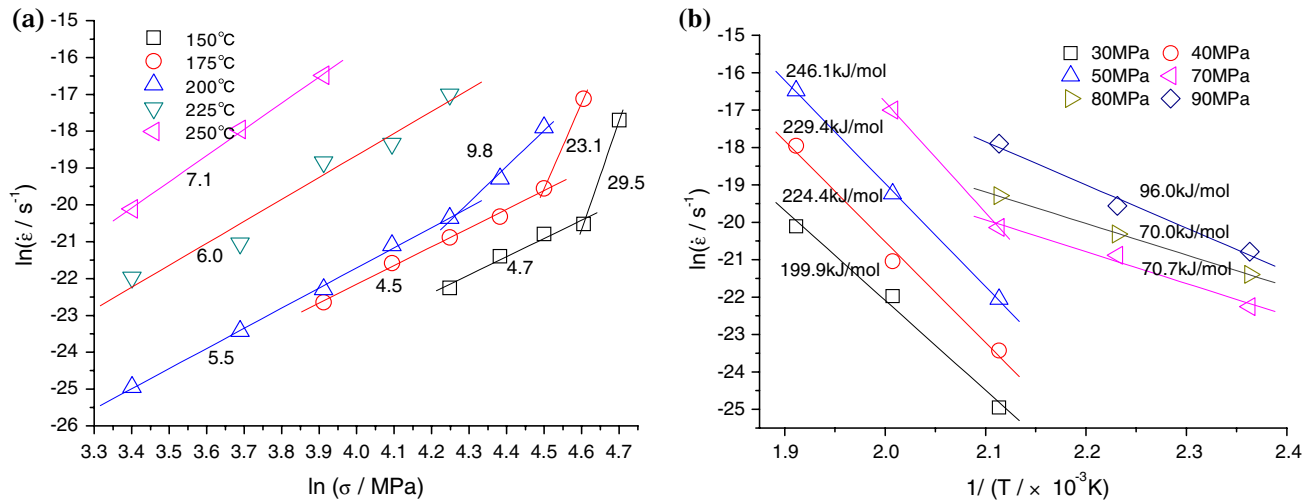

Fig. 4 (**a**) Stress and (**b**) temperature dependence of the steady-state creep rate of as-cast Mg-2Nd alloy

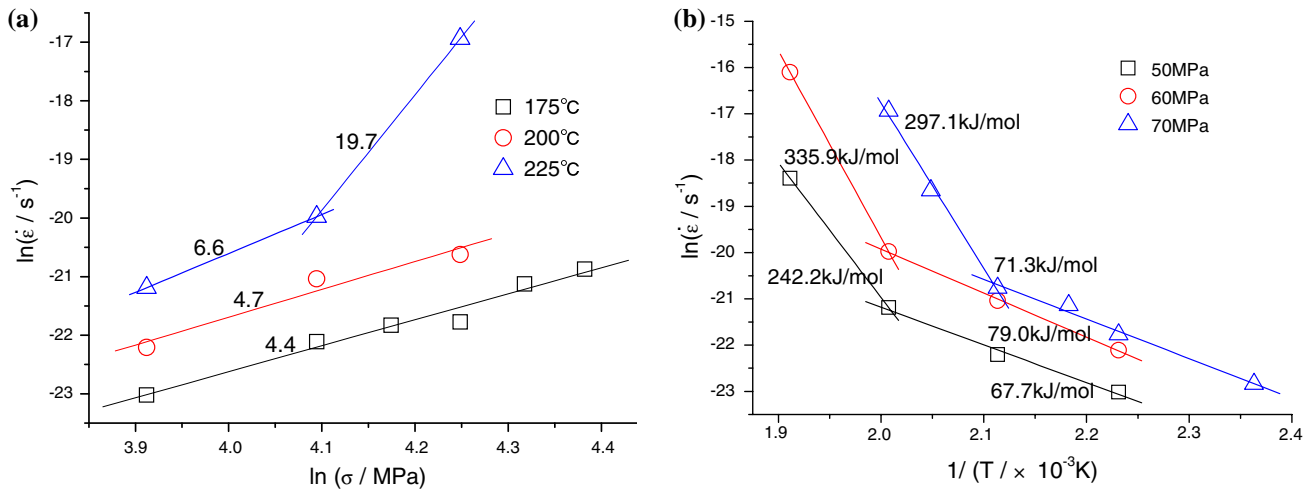

Fig. 5 (**a**) Stress and (**b**) temperature dependence of the steady-state creep rate of as-cast AJC421 alloy

at low stresses, but 19.7 at high stresses. The apparent activation energy for creep can also be divided into two parts: 67.7–79.0 kJ/mol at low temperatures and 242.2–335.9 kJ/mol at high temperatures, as shown in Fig. 5b.

Extrusion has different effect on the creep properties of the alloys Mg-2Nd and AJC421. The changes of creep properties of the alloys Mg-2Nd and AJC421 caused by extrusion are much different. The creep curves obtained from the as-extruded specimens of these two alloys at the temperature of 175 °C and a constant stress of 70 MPa are shown in Fig. 6. The steady-state creep rates and 100 h total creep extensions are listed in Table 2 together with those obtained from the as-cast specimens. It can be seen that the steady-state creep rate as well as the 100 h total creep extension of as-extruded Mg-2Nd specimen is a bit lower than those of as-cast specimen, indicating that the change of the second phase distribution and size of the matrix grain have no notable effect on the creep properties. For alloy AJC421, however, the steady-state creep rate of the as-extruded specimen is as high as 3.3×10^{-7} s^{-1}, which is three orders of magnitude higher than that of as-cast one (3.5×10^{-10} s^{-1}). The total creep extension increases by more the two orders of magnitude after extrusion. This sharp reduction of creep properties after extrusion implies that the morphology and distribution of intermediate phases in this alloy are main factors controlling the creep deformation.

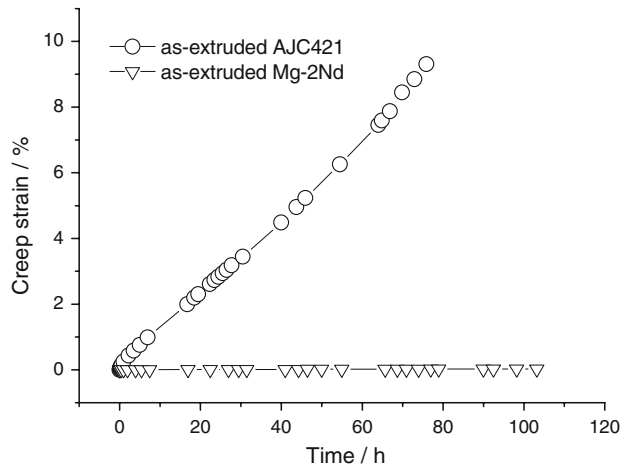

Fig. 6 Creep curves of the as-extruded Mg-2Nd and AJC421 at 175 °C/70 MPa

Figure 7a shows the SEM micrograph of as-cast Mg-2Nd alloy after creep test. In Mg-2Nd specimen, the interdendritic compounds ($Mg_{12}Nd$) distributed granularly instead of those in the microstructure before creep. The cracks are distributing along the grain boundaries but cavities exist both in the grains and along the grain boundaries. A large number of tiny needle-shaped

Table 2 Creep properties of as-cast and as-extruded alloy at 175 °C with applied stress 70 MPa

	Mg-2Nd		AJC421	
	As-cast	As-extruded	As-cast	As-extruded
Steady creep rate ($\dot{\varepsilon}$, s^{-1})	8.5×10^{-10}	6.1×10^{-10}	3.5×10^{-10}	0.078
100 h total creep extension (ε_t, %)	0.043	0.027	3.3×10^{-7}	9.31[a]

[a] This data was obtained after 76 h creep test as the specimen fractured

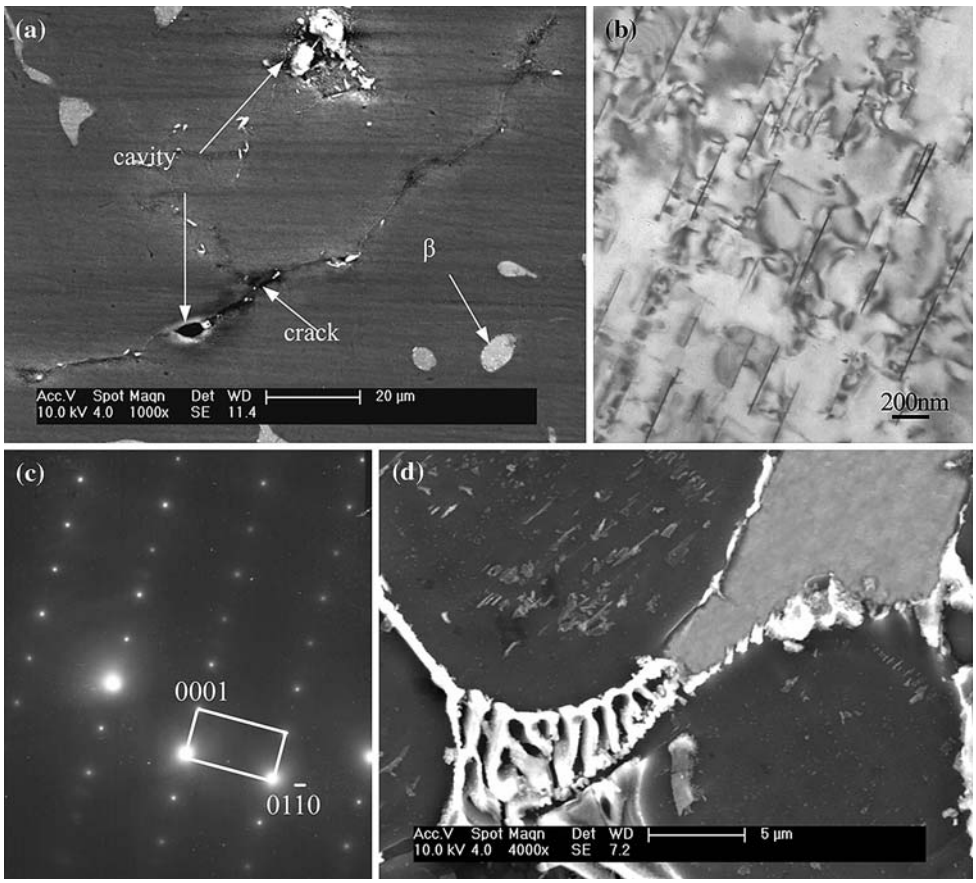

Fig. 7 (**a**) SEM micrograph of Mg-2Nd, (**b**) Precipitations, and (**c**) corresponding selected area diffraction pattern (B = $2\bar{1}\bar{1}0$) in Mg-2Nd after crept at 200 °C/70Mpa for 538 h, (**d**) SEM micrograph of AJC421 after creep test at 175 °C/ 70Mpa for 100 h

precipitations with the size of about 300–400 nm are visible and have interaction with the dislocations, as shown in Fig. 7b. Select area diffraction pattern (Fig. 7c) indicates the precipitations are parallel to the basal plane. Figure 7d shows the SEM micrograph of as-cast AJC421 alloy after creep test. The microstructure is nearly the same as that before creep test, indicating that the interdendritic compounds network is much stable during creep.

Discussion

Strengthening of the alloys

The previous investigations indicate that the mechanism for creep is either grain boundary sliding (or migration) or dislocation motion (climb or cross-slip) controlled [1]. Thus, the creep resistance of magnesium alloys can be improved by strengthening the grain boundaries or restricting the movement of dislocations. The improved mechanical properties through RE additions have been attributed to solution hardening and precipitation hardening, and particularly the precipitation of a fine dispersion of intermetallic particles [5, 12]. According to the Mg–Nd binary phase diagram [13, 14], the solubility of the neodymium in the α-Mg matrix is as high as 3.6wt% at 552 °C and decreases sharply with the decrease of temperature. At the ambient temperature the solubility of Nd in the α-Mg matrix is negligible. Due to non-equilibrium solidification the α-Mg in the alloy studied is oversaturated and part of neodymium forms divorced eutectic $Mg_{12}Nd$ instead of precipitates in the as-cast alloy. During creep tests, however, the tiny precipitates form from the oversaturated matrix, which are stable and effectively restrict the movement of dislocations. As a result, the as-cast Mg-2Nd alloy shows good creep resistance.

For most Mg–Al based alloys, such as AZ and AE series, discontinuous precipitation of the β phase ($Mg_{17}Al_{12}$) is thought to have deleterious effect on the creep properties of magnesium alloys [3]. The additions of alkaline earth elements strontium (Sr) and calcium (Ca) into Mg–Al alloys suppress the precipitation of $Mg_{17}Al_{12}$ and cause the formation of thermal-stable compounds (Mg–Al–Sr ternary phases and lamellar Mg_2Ca or $(Mg, Al)_2Ca$ phases) distributing along the grain boundaries. The thermal-stable compounds enable effective restriction to grain boundary sliding and migration so that the as-cast AJC421 alloy exhibits good creep resistance.

Creep mechanism

In the previous investigations, the stress exponent n and apparent activation energy Q parameters obtained from power-law equation

$$n = \left.\frac{\partial \ln \dot{\varepsilon}}{\partial \ln \sigma}\right|_{T=\text{constant}} \quad (3)$$

$$Q_c = -R \cdot \left.\frac{\partial \ln \dot{\varepsilon}}{\partial (1/T)}\right|_{\sigma=\text{constant}} \quad (4)$$

are usually used to infer the dominant creep deformation mechanisms in specific ranges of stress and temperature [1, 9, 10]. It is usually regarded that a stress exponent value of 1 is due to diffusion creep, 2 due to grain boundary sliding, and, 3–6 due to the motion of dislocations [1, 15]. An activation energy value of $Q_c = 30$–45 kJ/mol obtained in Mg–Al-based alloys (AZ91D,AS21 and AE42) [16] is reported to fit with the activation energy for discontinuous precipitation of $Mg_{17}Al_{12}$ which results in grain boundary sliding. A value of 80 kJ/mol is reported for grain boundary diffusion, 135 kJ/mol for self-diffusion, and 143 kJ/mol for diffusion of Al in Mg [3, 17].

In the present study, the obtained stress exponent values varying from 4.5 to 5.5 at low stresses at the temperatures between 150 and 200 °C lie in the range of 4–6, which is consistent with the five power law [18, 19] suggesting a dislocation climb controlled creep. The higher stress exponent values of 9.8–29.5 at higher stresses means power-law breakdown. However, the apparent activation energies lying between 70.0 and 96.0 kJ/mol at lower temperatures (150–200 °C) does not match the activation energy for self-diffusion, i.e., $Q_{sd} = 135$ kJ/mol, which is usually thought to be the activation energy for dislocation climb controlled creep [19, 20]. In some previous investigations on magnesium [17, 21–24], the authors still attributed the creep to be dislocation climb controlled based on the obtained stress exponents of 4.5–5.86 and activation energies of 92–117 kJ/mol, but few interpretations were given on the low activation energies. Nabarro [25], Sherby, and Weertman [26] suggested that the low activation energy was that for diffusion along the cores of dislocations which usually had nearly the same value as that for grain boundary diffusion. A decrease in activation energy from high temperature to low temperature has been found in many Mg-RE-based alloys [5, 12, 27]. The operative mechanism was still interpreted to be dislocation climb at low temperatures and the low activation energy was regarded as that of diffusion of vacancies [5]. A large number of tiny needle-shaped precipitations are visible and have interaction with the dislocations in the microstructure after creep test (Fig. 7b); indicating that the restriction effect of precipitates on the movement of dislocations is the main strengthening mechanism for good creep resistance. After extrusion the microstructure of the Mg-2Nd alloy is greatly refined due to dynamic recrystallization, as shown in Fig. 1d; however, the creep resistance of as-extruded sample is a bit better than that of as-cast sample, reflecting that grain boundary sliding (or migration) is not the controlling mechanism for creep. At high temperatures above 200 °C, higher stress exponents of 6.0 and 7.1 were obtained at 225 °C and 250 °C, respectively, while the apparent activation energies lie in the range from 199.9 kJ/mol to 246.1 kJ/mol. B.L.Mordike proposed: "The stress dependence of the activation energy would suggest it is probably the cross-slip mechanism" [5]. Suzuki et al. [28] obtained a high activation energy over 230 kJ/mol and observed cross-slip of dislocations from the basal to the non-basal plane in Mg-Y binary alloys, which was explained consistently by the cross-slip mechanism.

In the as-cast AJC421 alloy (Figs. 5a and b), the stress exponents are 4.4 and 4.7 at the temperatures of 175 °C and 200 °C, respectively, but 6.6 at low stresses and 19.7 at higher stresses at 225 °C. The apparent activation energies range from 67.7 kJ/mol to 79.0 kJ/mol at low temperatures (150–225 °C) and 242.2–335.9 kJ/mol at high temperatures (200–250 °C). According to the widely accepted criterion as described above, the creep at low temperatures and low stresses seems to be dislocation climb controlled since the stress exponents are close to 5, which is consistent well with the five power law. However, the apparent activation energy values range from 67.7 kJ/mol to 79.0 kJ/mol, close to that for grain boundary diffusion, much lower than that for self-diffusion. There have been few data reported concerning the stress exponent and activation energy for creep of Mg–Al–Sr–Ca alloys. Zhao et al. [29] attributed the low activation energy of 74 kJ/mol at low temperatures in Mg–Al–Sr alloy to grain sliding accommodated by grain boundary diffusion. Actually, grain sliding has been found to play an important role in the creep of Mg–Al-based alloys such as AZ91, AS21, and AE42 due to the creep-induced precipitation of β-$Mg_{17}Al_{12}$ [1, 3, 16]. Our previous work [6] reported that the creep properties of the AJC421 alloy, under the condition of 175 °C and 70 MPa, were three orders of magnitude higher than that of Mg-4Al binary alloy without Ca or Sr addition. As mentioned above, the remarkable improvement on creep resistance of the Mg–Al-based alloys is attributed to the elimination of discontinuous precipitation of β and formation of a network consisting of (Mg, Al)-Ca intermediate phases at grain boundaries, which are effective in restricting grain boundary migration. As soon as this network is damaged, the creep resistance drops rapidly. This can be clearly seen by comparing the creep properties of as-cast and as-extruded samples of the alloy AJC421, shown in Table 2. After extrusion, the intermediate phase

network was entirely destroyed, as shown in Fig. 2, leading to the sharp decrease of creep resistance. Under the condition of 175 °C and 70 MPa, the steady-state creep rate of the extruded sample is 3.7×10^{-7} s^{-1}, three orders of magnitude higher than that of as-cast sample, which is only 3.3×10^{-10} s^{-1}. Therefore, it seems that the creep behavior of the alloy is related mainly to grain boundary structure and hardly to say that it is controlled by dislocation movement. On the other hand, the apparent activation energies range from 67.7 kJ/mol to 79.0 kJ/mol at low temperatures (150–225 °C), close to the value for grain boundary diffusion. It seems, therefore, that the five power law might not be used to predict the creep mechanism for this alloy. To understand the mechanism responsible for creep of different magnesium alloys, further study is needed.

Conclusion

1. Both as-cast Mg-2Nd and AJC421 alloys exhibited good creep resistance in comparison with commonly used magnesium alloys.
2. The improvement of creep properties through Nd addition to pure magnesium is attributed to both solid solution and precipitation hardening. The stress exponents of 4.5–5.5 and activation energies of 70.0–96.0 kJ/mol obtained from the as-cast Mg-2Nd alloy at low temperatures and low stresses indicates the five power law can be used for predicting the creep mechanism.
3. The additions of alkaline earth elements Sr and Ca into Mg–Al alloys suppress the precipitation of $Mg_{17}Al_{12}$ and form thermal-stable compounds at the grain boundaries, leading to effective restriction to grain boundary sliding and migration. However, the mechanism responsible for creep deformation of Mg–Al-based alloys with Ca and Sr additions is not consistent with the results of microstructure observations performed on the alloys before and after creep tests.

Acknowledgement This research was supported by the Natural Science Foundation of Jiangsu Province (No. BK2004208) and the Foundation for Excellent Doctoral Dissertation of Southeast University.

References

1. Luo AA (2004) Int Mater Rev 49:13. doi:10.1179/095066004225010497
2. Lu YZ, Wang QD, Zeng XQ et al (2000) Mater Sci Eng A 278:66. doi:10.1016/S0921-5093(99)00604-8
3. Pekguleryuz MO, Kaya AA (2003) Adv Eng Mater 5:866. doi:10.1002/adem.200300403
4. Blawert C, Hort N, Kainer KU (2004) Trans Indian Inst Metab 57:397
5. Mordike BL (2002) Mater Sci Eng A 324:103. doi:10.1016/S0921-5093(01)01290-4
6. Bai J, Sun YS, Xue S et al (2006) Mater Sci Eng A 419:181. doi:10.1016/j.msea.2005.12.017
7. Sherby OD, Burke PM (1968) Prog Mater Sci 13:323. doi:10.1016/0079-6425(68)90024-8
8. Couret A, Caillard D (1985) Acta Mater 33:1447. doi:10.1016/0001-6160(85)90045-8
9. Evangelista E, Gariboldi E, Lohne O et al (2004) Mater Sci Eng A 387–389:41. doi:10.1016/j.msea.2004.02.077
10. Evans RW, Wilshire B (1985) Creep of metals and alloys. The Institute of Metals, New York
11. Xue S, Sun YS, Zhu TB et al (2005) Trans Nonferr Met Soc 15:863
12. Wang JG, Hsiung LM, Nieh TG et al (2001) Mater Sci Eng A 315:81. doi:10.1016/S0921-5093(01)01209-6
13. Nagasaki S, Hirabayashi M (2002) Binary alloy phase-diagrams. AGNE Gijutsu Center Co Ltd, Tokyo
14. American Society for Metals (1973) Metals handbook. Metals Park, Ohio
15. Nabarro FRN (2007) Encyclopedia of materials: science and technology. Elsevier Science Ltd, Oxford, p 1788
16. Dargush MS, Dunlop GL, Pettersen K (1998) In Mordike BL, Kainer KU (eds) Proceedings volume sponsored by Volkswagen AG. Werkstoff-Informationsgesellschaft, Frankfurt, p 277
17. Shi L, Northwood DO (1994) Acta Metall Mater 42:871. doi:10.1016/0956-7151(94)90282-8
18. Kassner ME, Kumar P, Blum W (2007) Int J Plast 23:980. doi:10.1016/j.ijplas.2006.10.006
19. Kassner ME, Pérez-Prado M-T (2004) Fundamentals of creep in metals and alloys. Elsevier Science Ltd, Oxford
20. Weertman J (1957) J Appl Phys 28:362. doi:10.1063/1.1722747
21. Jones RB, Harris JE (1963) Joint international conference on Creep, Part 3A. Inst Mech Eng Proc, NewYork
22. Tegart WJ (1961) Acta Metall 9:614. doi:10.1016/0001-6160(61)90166-3
23. Crossland IG, Jones RB (1972) Met Sci J 6:162
24. Crossland IG, Jones RB (1977) Met Sci J 11:504
25. Nabarro FRN (1967) Philos Mag 16:231. doi:10.1080/14786436708229736
26. Sherby OD, Weertman J (1979) Acta Metall 27:387. doi:10.1016/0001-6160(79)90031-2
27. Mordike BL, Stulikova I (1983) In: Proceedings of the international conference on metallic light alloys. Institution of Metallurgists, London, p 146
28. Suzuki M, Sato H, Maruyama K et al (2001) Mater Sci Eng A 319–321:751. doi:10.1016/S0921-5093(01)01005-X
29. Zhao P, Wang QD, Zhai CQ et al (2007) Mater Sci Eng A 444:318. doi:10.1016/j.msea.2006.08.111